



UNIVERSITY OF LEEDS

This is a repository copy of *Exploring the features on the OH + SO₂ potential energy surface using theory and testing its accuracy by comparison to experimental data.*

White Rose Research Online URL for this paper:
<http://eprints.whiterose.ac.uk/129263/>

Version: Accepted Version

Article:

Medeiros, DJ, Blitz, MA orcid.org/0000-0001-6710-4021 and Seakins, PW (2018)
Exploring the features on the OH + SO₂ potential energy surface using theory and testing its accuracy by comparison to experimental data. *Physical Chemistry Chemical Physics*, 20 (13). pp. 8984-8990. ISSN 1463-9076

<https://doi.org/10.1039/c8cp00091c>

This is an author produced version of a paper published in *Physical Chemistry Chemical Physics*, © the Owner Societies 2018. Uploaded in accordance with the publisher's self-archiving policy.

Reuse

Items deposited in White Rose Research Online are protected by copyright, with all rights reserved unless indicated otherwise. They may be downloaded and/or printed for private study, or other acts as permitted by national copyright laws. The publisher or other rights holders may allow further reproduction and re-use of the full text version. This is indicated by the licence information on the White Rose Research Online record for the item.

Takedown

If you consider content in White Rose Research Online to be in breach of UK law, please notify us by emailing eprints@whiterose.ac.uk including the URL of the record and the reason for the withdrawal request.



eprints@whiterose.ac.uk
<https://eprints.whiterose.ac.uk/>

Exploring the features on the OH + SO₂ potential energy surface using theory
and testing its accuracy by comparison to experimental data

D.J. Medeiros,^a M.A. Blitz,^{a,b*} and P.W. Seakins^{a,b}

^a *School of Chemistry, University of Leeds, Leeds, LS2 9JT, UK*

^b *National Centre for Atmospheric Science, University of Leeds, Leeds, LS2 9JT, UK*

*E-mail: m.blitz@leeds.ac.uk

Abstract

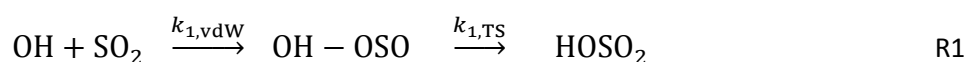
Ab initio theory has been used to identify the pre-reaction complex in the atmospherically important reaction between OH + SO₂, R1, where the binding energy of the pre-reaction complex was determined to be 7.2 kJ mol⁻¹. Using reaction rate theory, implemented with the master equation package MESMER, the effects of this complex on the kinetics of R1 at temperatures above 250 K have been investigated. From simulations and fitting to the experimental kinetic data, it is clear that the influence of this pre-reaction complex is negligible and that the kinetics are controlled by the inner transition-state that leads to the product, HOSO₂. While the effect of this complex on the thermal kinetics is small it potentially provides an efficient route to remove energy from vibrationally excited OH. The fitting to the past experimental data reveals that this inner transition-state is submerged with a barrier -0.25 kJ mol⁻¹ below the entrance channel, which is outside the range predicted from the best theoretical calculations. The data fitting also yielded $\Delta_{R1}H_{0K}$ equal to $-(109 \pm 5.6)$ kJ mol⁻¹ and a more precise expression for $k_1^\infty(T)$, $(5.95 \pm 0.83) \times 10^{-13} \times (T/298)^{-0.11 \pm 0.27}$.

1. Introduction

Sulphur dioxide, SO_2 , plays a major role in the atmosphere; its reaction with the hydroxyl radical:



ultimately leads to sulphuric acid via subsequent reactions of HOSO_2 with O_2 and H_2O , where sulphuric acid contributes significantly to new particle formation.^{1, 2} Recently, experimental studies were used to determine the limiting high-pressure rate coefficient for reaction R1, $k_1^\infty(T)$,³ and values for $k_1(T,p)$ over a wide range of conditions.⁴ These studies highlighted the difficulties in obtaining reliable parameters on this reaction, and in order to assign the limiting high-pressure limit, the analysis implied that a weakly bound pre-reaction complex, $\text{OH}-\text{OSO}$, was present, see Figure 1:



where $k_{1,\text{vdW}}$ is the rate coefficient for formation of the pre-reaction complex, vdW, and $k_{1,\text{TS}}$ is the rate coefficient for product formation, HOSO_2 , from the vdW, see Figure 1. It was after these papers were published that this pre-reaction complex was identified from theoretical calculations.⁵ However, these calculations were carried out at a relatively low level and the crucial barrier height between the pre-reaction complex and HOSO_2 is poorly defined. Also, recently, the $\text{OH} + \text{SO}_2$ potential energy surface, but not including the pre-reaction complex, has been calculated at beyond-CCSDT correlation energies and this result was used to theoretically predict $\text{OH} + \text{SO}_2$ rate coefficients.⁶ From this study, k_1^∞ at 298 K was calculated to be $1.3 \times 10^{-12} \text{ cm}^3 \text{ molecule}^{-1} \text{ s}^{-1}$, which is considerably higher than the experimentally determined value: $(7.2 \pm 3.3) \times 10^{-13} \text{ cm}^3 \text{ molecule}^{-1} \text{ s}^{-1}$.⁴ However, the main difference between these two studies is associated with the temperature dependence of k_1^∞ ; the theoretical study assigns a barrier to reaction R1 of 1.1 kJ mol^{-1} ⁶ while the experimental studies observe no increase in k_1^∞ with temperature and assign a negative activation energy for reaction.^{3, 4}

In this report we investigate the potential effect of this pre-reaction complex^{7, 8} to see if it can reconcile the results of this theoretical description of the reaction with the experimental data, where reaction rate theory, the master equation programme MESMER,^{9, 10} is used to perform the modelling and fitting. In addition, this master equation analysis identifies the energy of the transition-state controlling the reaction, the binding energy of the reaction product, HOSO_2 , and better defines $k_1(p,T)$.

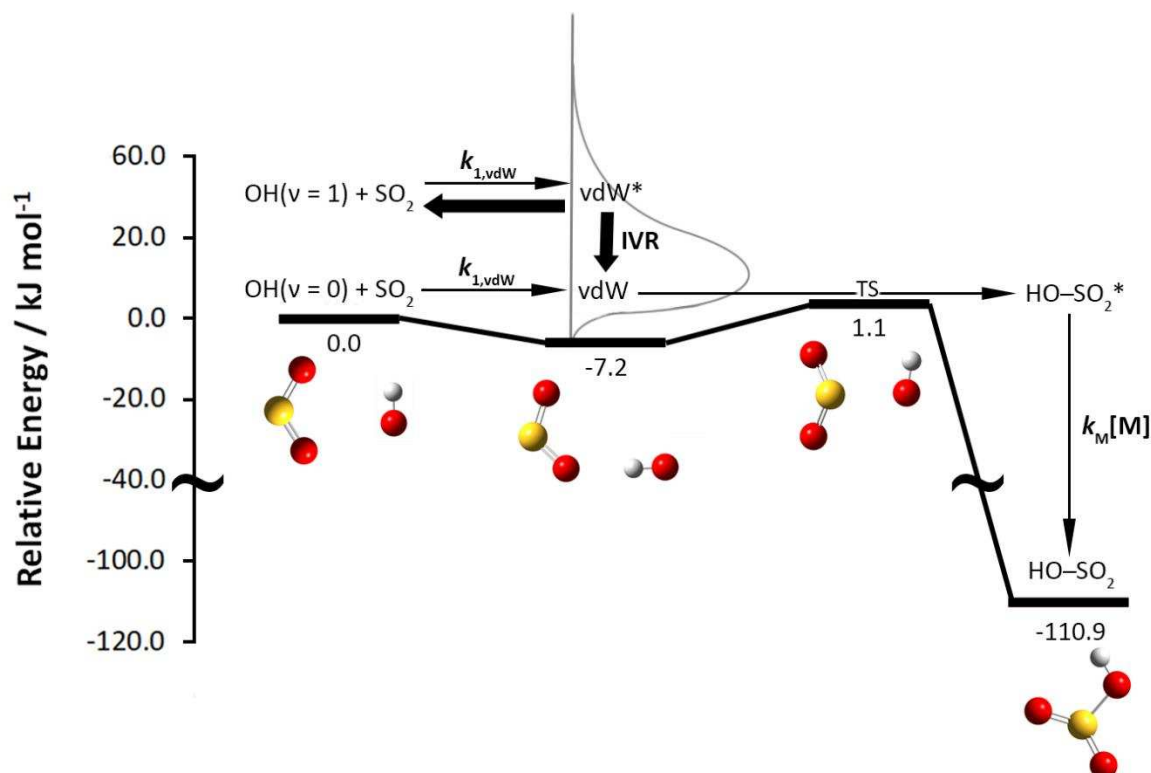


Figure 1. Potential energy diagram for the reaction between OH and SO₂, where a weakly bound complex, vdW, is formed before proceeding over the transition-state, TS, to products, HOSO₂. The energies of the stationary states are those calculated in this work, with zero point energies added. Also included is OH(*v*=1) + SO₂ reaction, which initially forms a “hot” vdW(**) that either re-dissociates back to reagents or undergoes intramolecular energy redistribution (IVR) to vdW(*), which does not significantly re-dissociate to OH(*v*=1) + SO₂; the two thick arrows indicate that these processes are in competition. The Boltzmann energy distribution of the vdW is illustrated; it resides above the binding energy of this complex.

2 Computational methods

Ab Initio calculations were undertaken to determine molecular properties of the relevant species which were implemented in subsequent master equation calculations^{11, 12} using the MESMER package.¹¹ Stationary points of the involved species were calculated with the DFT functional M06-2X¹³ and the aug-cc-pVQZ basis set.¹⁴⁻¹⁸ Molecular structures were optimized with the aid of the Gaussian 09 D.01 software¹⁹ using analytic gradients and the Beryny algorithm²⁰ in redundant internal coordinates. Single point energies (SPE) of the M06-2X/aug-cc-pVQZ optimized geometries were computed via coupled cluster calculations with single, double and triple excitations, the triples being described perturbatively (CCSD(T)).²¹ SPE results were extrapolated to the complete basis set limit (CBS) using the extrapolation scheme presented by Peterson *et al.*¹⁷ and Dunning’s correlation consistent basis sets (aug-cc-pVXZ, X=D, T, Q). Harmonic vibrational frequencies, rotational constants, force-constant matrices and zero-point energies (ZPE) were calculated at the M06-2X/ aug-cc-pVQZ level. The hindered rotor approach was used to describe the internal rotation around the O₂S-OH

bond. The potential was mapped out via a relaxed scan of the dihedral angle with respect to this rotation, with 24 steps of 15°. A restricted structure optimization of the molecule at the M06-2X/ aug-cc-pVQZ level of theory was performed for each step of the scan. Using this description of a hindered rotor, MESMER uses the procedure presented by Sharma *et al.*²² to project out the respective vibrational modes.

One of the most versatile methods for modelling pressure dependent reactions is the energy grained master equation method (EGME), which is described in general terms by equation E1:

$$\frac{dp}{dt} = \mathbf{M}p \quad \text{E1}$$

where \mathbf{M} , the transition matrix, describes the temporal evolution of the population due to collisional energy transfer and chemical reaction and p is the population density vector. In setting up E1, energy levels for each species of the system (reagents, intermediates and products) are grouped into grains of typically 50 cm⁻¹, and E1 describes a set of differential equations that links the grains of these species. Energy transfer brings about population/depopulation of each energy grain via its collision with the buffer gas, and is described in the current EGME by an exponential down model, where the probability of energy transfer, $\langle \Delta E_d \rangle$, is reduced exponentially as a function of the separation of the two grains. Detailed balance ensures a Boltzmann distribution is obtained in the absence of chemical reaction. Also in the current EGME, the comparison of experimental data generated with different bath gases is possible, since the energy transfer parameter, $\langle \Delta E_d \rangle$, can assume a different value for each gas. Chemical reaction between the energy grain species is described via microcanonical rate constants, which in the case of reaction with a defined transition-state are calculated via RRKM theory.²³ When there is no barrier (saddlepoint) to reaction the microcanonical rate constants are calculated using Inverse Laplace Transformation (ILT)²⁴ of $k^\infty(T)$, where knowledge of $k^\infty(T)$ may be known from experiments.

The solution of E1 has the form of E2:

$$p = \mathbf{U}e^{\Lambda t}\mathbf{U}^{-1}p(0) \quad \text{E2}$$

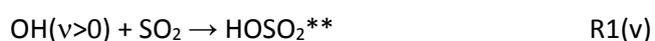
where $p(0)$ contains the initial conditions for the grains, \mathbf{U} is a matrix of eigenvectors obtained via diagonalization of \mathbf{M} and Λ is the vector of the accordant eigenvalues. MESMER solves the EGME and the phenomenological rate coefficients are selected from the chemically significant eigenvalues using the Bartis-Widom procedure.²⁵ When considered, quantum mechanical tunnelling corrections are done with the use of an unsymmetrical Eckart barrier, following the procedure reported by Miller *et al.*²⁶

3 Results and Discussion

The stationary points on the potential energy surface of reaction R1 were identified and are shown in Figure 1 and their energies are given in Table 1. A van der Waals (vdW) pre-reaction complex was identified and was calculated to be 7.2 kJ mol⁻¹ below the entrance channel. This vdW complex was recently identified by Miriyala *et al.*,⁵ but using a lower level of theory calculation, MP2/aug-cc-pVTZ.

The recent calculations of Long *et al.*,⁶ Klopper *et al.*²⁷ and the present calculation are in good agreement with experiment²⁸ with respect to $\Delta_R H_{R1}$, see Table 1; from 0 to 298 K adds about 5 kJ mol⁻¹ to the binding energy. The fact that Miriyala *et al.*⁵ calculates $\Delta_R H_{R1}$ in agreement with the other calculations would appear to be fortuitous as their barrier for the transition-state, TS, is very high, 22.2 kJ mol⁻¹. The value for TS from Long *et al.*⁶ and this study are 1.1 and 1.2 kJ mol⁻¹, respectively. The study by Long *et al.*⁶ is the highest level calculation and the present calculation is in good agreement with it. Therefore it is concluded that the values of Miriyala *et al.*⁵ are only semi-quantitative and their value of -17.6 kJ mol⁻¹ for the binding energy of the vdW complex would appear too large compared to our value of -7.2 kJ mol⁻¹.

The reason the vdW complex is important is because it can influence energy transfer processes between reagent species. In our previous study³ to determine k_1^∞ , the removal rate coefficients of vibrational excited hydroxyl radical (OH(v)) in the presence of SO₂ were determined:

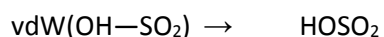


where HOSO₂** is the nascent product, where the ** indicates that it has additional energy from the vibrationally excited OH. Now HOSO₂** can be lost in a number of ways but it is unlikely to return to OH(v>0),²⁹ so the removal rate coefficient is a measure of the limiting high-pressure rate coefficient for reaction R1, k_1^∞ . This is known as the proxy method for determining the high-pressure rate coefficient, and was first proposed by Smith.³⁰ However, in our recent study, the removal rate coefficients, $k_1(v>0)$ were $> k_1^\infty$.³ In order to extract k_1^∞ our analysis implied another species on the R1 potential energy surface, i.e. OH—OSO, a vdW complex. In order to bring about efficient vibrational energy transfer the vdW complex has to have a significant lifetime, and if the lifetime is sufficiently long then the $k_1(v>0)$ would provide a proxy for the limiting high-pressure rate coefficient for vdW complex formation, which is reasonably expected to be close to the gas-kinetic collision frequency, $\sim 10^{-10}$ cm³ molecule⁻¹ s⁻¹, see Table 2 for estimates of the vdW complex capture rate coefficient, $k_{1,\text{vdW}}^\infty$. However, the measured values of $k_1(v)$ were much smaller than the gas-kinetic frequency and increased significantly with vibrational level.³ This implies that the lifetime of the complex is too short for the internal modes of the vdW to totally re-distribute the energy throughout the complex, but long enough for partial re-distribution, this is illustrated in Figure 1 for OH(v=1) + SO₂. The RRKM lifetime of this vdW complex is ~ 1 picosecond, and its population at $T > 250$ K is mainly above the barrier to products, HOSO₂, see Figure 1. Redistribution of energy throughout a molecule is known as intramolecular energy redistribution (IVR) and typically occurs on the femto to pico-second timescale,²⁹ therefore it is a possibility that IVR is incomplete before OH—OSO formed from OH(v) re-dissociates back to reagents. Whether the presence of this vdW complex on the R1 PES can quantitatively explain our $k_1(v)$ data³ is something to be determined in the future, but the magnitude and behaviour of $k_1(v)$ is qualitatively consistent with the vdW complex facilitating partial vibrational energy relaxation.

In the present study the effect of this vdW complex on the thermal rate coefficients, $k_1(p, T)$ is investigated using reaction rate theory, implemented with MESMER.⁹ The overall reaction R1 (see Figure 1) incorporates the formation of the vdW complex:



followed by further reaction over the inner transition-state to products:



R1,TS

Inverse Laplace Transformation (ILT) is a pragmatic method to calculate the microcanonical rate constants.²⁴ ILT is particularly useful for reactions where there is no barrier (saddlepoint) to reaction as it is not obvious where the transition-state is located. If the barrierless reaction of interest has been studied experimentally and its rate coefficient $k^\infty(T)$ determined, then ILT of $k^\infty(T)$ calculates the corresponding set of microcanonical rate constants. Typically, for a barrierless reaction $k^\infty(T)$ can be represented by the expression: $A(T/298)^n$. In the present analysis this representation is used for the ILT. More details on using ILT can be found in the MESMER manual.¹⁰ In the present MESMER calculation ILT is used to describe the formation of $\text{vdW}(\text{OH}-\text{SO}_2)$, via reaction R1, $k_{1,\text{vdW}}$. This is a barrierless reaction, see Figure 1, and while there are no experimental rate coefficients it is reasonable to assume that $k_{1,\text{vdW}}^\infty$ is fast and close to the gas-kinetic collision frequency. This is borne out in the analysis, see Table 2. RRKM theory²³ is used to calculate microcanonical rate constants over the inner transition-state, $k_{1,\text{TS}}$, where there is a defined barrier (saddlepoint) to products. These coupled reactions R1,vdW and R1,TS are solved within MESMER, together with the energy transfer processes, in order to generate $k_1(p,T)$.⁹ These calculated rate coefficients are regressed (adjusted parameters are given in Table 2) to best fit the experimental data.

In our previous study on the thermal rate coefficients much of the literature was not used in the final assessment as it could not be reconciled.⁴ These unreconciled data could be attributed to unwanted chemistry arising from SO_2 photolysis perturbing the observed kinetics and included data that indicated R1 had a positive temperature dependence.³¹ In the present MESMER analysis we use just the reconciled data, see the supporting information, ESI. In addition, the current analysis included high temperature dissociation data, $k_{-1}(p,T)$, from Blitz *et al.*²⁸ where OH was in equilibrium with SO_2 . These data were not used in our previous analysis.⁴ Including these data decreases the uncertainty in $k_1(p,T)$, see Figure 2. When the Blitz *et al.*²⁸ study was carried out the nature of SO_2 photolysis was unknown. However, an “unknown” bimolecular OH loss channel was included in the analysis, and this can now be reasonably interpreted as reaction between OH and the SO_2 photolysis products. However, there is still considerable uncertainty in the $k_1(p,T)$ data from this study, so these data are not included in the current analysis. The $k_{-1}(p,T)$ data should be reliable as it is unimolecular and depends strongly on temperature and is not strongly affected by SO_2 photolysis products. Re-analysis of this data confirms this assertion.

Reaction R1 according to Figure 1 is not a single step but is made up of the reactions R1,vdW and R1,TS. When the reaction is more than a single step it is safest to assume that the measured kinetic data are simply the total removal of OH rather than assume it is OH reacting to HOSO_2 . So in the MESMER analysis the literature data are assigned as the total loss of OH in the presence of SO_2 , and the total loss of HOSO_2 in the case of the high temperature data. Experiments measure phenomenological rate coefficients,³² which correspond to eigenvalues of the kinetic matrix, assuming the underlying abstract model is correct. The eigenvalue might be equal to a single step rate coefficient in the case of a simple reaction, but it might be a mixed rate coefficient for a reaction like R1, i.e. a combination of $k_{1,\text{vdW}}$ and $k_{1,\text{TS}}$. A good example of a complex reaction is the reaction between OH + CH_3OH , which at room temperature appears to be a single step but is revealed to be complex as the rate coefficient at very low temperatures ($T < 100$ K) dramatically increases and is controlled almost exclusively by the pre-reaction complex.³³

Several models were considered when performing the MESMER data analysis and the results are summarized in Table 2. The first case considered all the species in Figure 1 and described the 3n-6 vibrations as harmonic oscillators, model A; a rigid rotor harmonic oscillator model. From model A, it is observed that the rate coefficient for the formation the vdW complex, $k_{1,\text{vdW}}$, is fast and ill-defined, $(1.6 \pm 1.9) \times 10^{-10} \text{ cm}^3 \text{ molecule}^{-1}\text{s}^{-1}$. This implies that the reaction is wholly controlled by the inner transition-state, TS. The energy of the TS is slightly negative ($-0.38 \text{ kJ mol}^{-1}$) compared to the entrance channel, which implies the overall rate coefficient is going to decrease as temperature is increased. The submerged barrier returned by model A contrasts with the slight positive barrier from the *ab initio* calculations, see Table 1. In model B, $k_{1,\text{vdW}}$ is fixed to the value from model A and returns only slightly reduced errors in the parameters. This is further evidence that the vdW complex has little effect on the kinetics over the temperature range of the data, i.e. $k_{1,\text{vdW}}$ is not coupled to the other parameters and this is borne out from the correlation matrix of Model A. Models A and B return Δ_{R1H0K} equal to -112 kJ mol^{-1} .

A potential problem with describing the 3n-6 vibrations as harmonic oscillators is that they have degrees of anharmonicity, and the degree of anharmonicity is much higher for the low frequency vibrations. This problem manifests itself as incorrectly calculating density of states and hence the entropy of the reaction, $\Delta_{\text{R}}S$, which in turn affects the value assigned to the enthalpy of the reaction, $\Delta_{\text{R}}H$. This is a problem as theory calculates the 0 K enthalpy of reaction, Δ_{R1H0K} , but experimental values are determined at temperatures 100s K higher, e.g. 563 K in the case of $\Delta_{\text{R1H}}(\text{HOSO}_2)$ from Blitz *et al.*²⁸ Experiments and theory attempt to compare Δ_{R1H0K} , but for this to be a like-for-like comparison, the internal motions of the molecules need to be described accurately. A better way to account for the low frequency bend and torsional vibrations is to describe them as hindered rotors. In the hindered rotor models of Table 2, the hindered rotation around the HO—SO₂ bond has been calculated and used in the MESMER calculation; this hindered rotation mode is projected out of the Hessian using the method reported by Sharma *et al.*²² rather than removal of the corresponding vibration. In Model C where a hindered rotor is considered for the HO—SO₂ bond, then, as expected, the vdW capture rate coefficient, $k_{1,\text{vdW}}$, is fast and ill-defined, $(1.3 \pm 5.9) \times 10^{-10} \text{ cm}^3 \text{ molecule}^{-1}\text{s}^{-1}$. When this capture rate coefficient is fixed, model D, the errors in the returned parameters are little reduced. This indicates that vdW complex is not playing a significant role in the kinetics; the same conclusion when comparing Models A and B. The energy of the TS is again slightly negative, $(-0.24 \pm 0.10) \text{ kJ mol}^{-1}$, and in agreement with the vibrational only description of the system, model B. The effect of including a hindered rotor is observed in the returned value for Δ_{R1H0K} is $(-108.9 \pm 0.7) \text{ kJ mol}^{-1}$, which is $\sim 3 \text{ kJ mol}^{-1}$ less than the vibrational model, B. This difference arises mainly because model D ($\Delta_{\text{R1S298K}} = -137.5 \text{ J K}^{-1} \text{ mol}^{-1}$) has a lower entropy of reaction than model B ($\Delta_{\text{R1S298K}} = -143.7 \text{ J K}^{-1} \text{ mol}^{-1}$). In general, model D is a better description of the system than model B, so from MESMER fitting to the experimental data our recommended value for Δ_{R1H0K} is $(-108.9 \pm 0.7) \text{ kJ mol}^{-1}$.

From Table 2, it appears that Klopper *et al.*²⁷ is in best agreement with our recommended value for Δ_{R1H0K} based on the MESMER modelling of the experimental data. The more recent *ab initio* value from Long *et al.*⁶ is $-111.5 \text{ kJ mol}^{-1}$ and this is the highest level calculation. Our present calculation gives $-110.9 \text{ kJ mol}^{-1}$. So it would appear for present the system, the accuracy of *ab initio* calculation is no better than a few kJ mol^{-1} (-108.9 versus $-111.5 \text{ kJ mol}^{-1}$). However, the MESMER value of $(-108.9 \pm 0.7) \text{ kJ mol}^{-1}$ is dependent on the energy transfer parameters for helium, $\langle \Delta E_{\text{down,He}} \rangle = \Delta E_{\text{d,He}} \times (T/298)^m$, as this was the bath gas used for the equilibrium experiments.²⁸ The values for

$\langle \Delta E_{d,He} \rangle$ in Table 2 are consistent with values obtained for other systems,³⁴ and for model D the temperature dependence of $\langle \Delta E_{down,He} \rangle$ has been fixed to $(T/298)^{1.0}$. In model E the temperature dependence of $\langle \Delta E_{d,He} \rangle$ has been allowed to float, $(T/298)^m$, and returns a value for m close to unity (0.99 ± 1.52), but the returned parameters have increased errors. The value for $\Delta_{R1}H_{0K}$ from model E is (-109.1 ± 5.5) kJ mol⁻¹, which is essentially the same value as model D, but the errors are larger and probably represent a better overall estimate of how well $\Delta_{R1}H_{0K}$ is known. The correlation matrix from model E has m strongly correlated (almost unity) to $\Delta_{R1}H_{0K}$, where m increases with binding energy. Until more $k_1(p,T)$ are determined over a larger temperature range it is not possible to favour a particular theoretical study with good confidence.

Also from Table 2, it can be seen that the energy of the TS is always slightly negative compared to the entrance channel and is almost independent of the chosen models. Model E, where all the parameters are allowed to float returns an energy for the TS equal to (-0.24 ± 0.10) kJ mol⁻¹. This value with its errors is outside the values from the *ab initio* calculations. This indicates that the accuracy of these calculations is > 1 kJ mol⁻¹. While such accuracy from calculations is an achievement, a difference of 1 kJ mol⁻¹ does make a significant difference at room temperature when predicting rate coefficients. In model F, the energy of the TS is fixed to the value of Long *et al.* (1.1 kJ mol⁻¹ and very close to our calculated value of 1.2 kJ mol⁻¹)⁶ and from Table 2 it can be seen that χ^2/point , the goodness of fit, is twice that of the previous models, and in model G, where both the energies of the TS and $\Delta_{R1}H_{0K}$ are fixed to the values of Long *et al.*,⁶ the fit is worse. In the ESI, Figure S1 shows a plot of $k_1(\text{calculated})$ versus $k_1(\text{measured})$ for models E and G, where deviation from a slope equal to 1.0 indicates disagreement between the model and experiment, plus an inset plot of the model E fit to the experimental data versus buffer gas concentration. By fixing the energy of the TS to a positive value it cannot provide as good a fit to the data as models A – E. The possibility that the vdW complex might provide an explanation of the experimental data with a positive value for TS is discounted as the current MESMER analysis shows that for $T > 250$ K the kinetics of reaction R1 are almost exclusively controlled by the inner transition-state, TS.

The assumption in the MESMER analysis that includes the vdW complex, is that the inner transition-state, TS, is fixed as temperature (energy) is varied. This is a good approximation for reactions over significant barriers. But this is not the case here as the calculated barrier from the vdW complex to TS is only 8.2 kJ mol⁻¹. When the barrier is small or barrierless the transition-state moves as a function of energy;³⁵ generally becoming more adduct-like as temperature increases. However, this analysis has shown that at $T > 250$ K the vdW complex has essentially no influence and the kinetics are wholly controlled by the inner transition-state, TS. Therefore we can simply treat the reaction using one transition-state, where Inverse Laplace Transformation (ILT) parameters, $k_1^\infty \times (T/298)^n$, are used to calculate the microcanonical rate constants, and the value of n allows for the variation of the inner transition-state with temperature. The data have been modelled using this single transition-state, ILT model and the results are given in Table 2, model H. The energy transfer parameters are essentially unchanged from the other models and the value of n is -0.09 ± 0.27 , which is effectively equal to an E_a of -0.20 kJ mol⁻¹, i.e. consistent with the results from the vdW complex models. In Figure 2, k_1^∞ from model G is plotted as a function of temperature, together with our previous estimate of k_1^∞ from R1(v) analysis³ and the theoretical values of Long *et al.*⁶ From Figure 2, it can be seen that our previous study and the present analysis are in good agreement, with the present analysis better defining $k_1^\infty(T)$. The present values of $k_1^\infty(T)$ show a slight negative temperature dependence, which

is in stark contrast to the Long *et al.* values for k_1^∞ , which are increasing with temperature as a consequence of the 1.1 kJ mol⁻¹ barrier. The input file for the MESMER calculation are given in the ESI together with simple parameterized forms for $k_1(p,T)$ for helium, argon and nitrogen (similar to air) bath gases.

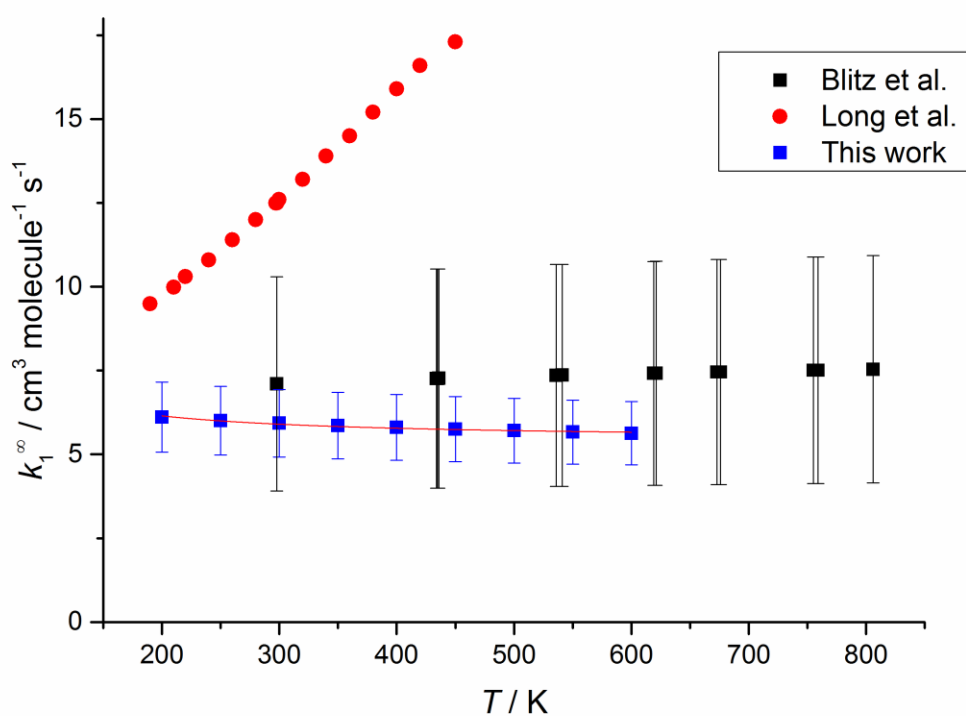


Figure 2. $k_1^\infty(T)$ determined in this work, Model H, Blitz *et al.*,³ using the removal rate coefficients of vibrational excited OH with SO₂, and the theoretical study by Long *et al.*⁶ The red line is an Arrhenius fit to the present data and yields an E_a /kJ mol⁻¹ equal to -0.20.

3 Conclusions

Calculations on the reaction between OH + SO₂, R1, reveal that on its potential energy surface a weakly bound van der Waals complex is initially formed, bound by 7.2 kJ mol⁻¹. In our previous paper on the removal of vibrationally excited hydroxyl with SO₂,³ a weakly bound van der Waals pre-reaction

complex was invoked to explain the data. Therefore these calculations confirm this prediction. The impact of this complex on kinetics of reaction R1 have been investigated using master equation analysis, implemented using MESMER, where the results are compared to the literature and the important parameters of the potential energy surface are suitably adjusted to best fit the literature, where $T > 250$ K. This analysis reveals that this pre-reaction complex has essentially no influence on the kinetics, and implies the rate coefficient is wholly controlled by the inner TS, see Figure 1. From the MESMER fitting to evaluated kinetic data, it is clear that the energy of the inner TS is negative compared to the entrance channel, -0.2 kJ mol⁻¹, and this is over a kJ mol⁻¹ lower than the best calculated value for TS. This MESMER analysis assigns a value for $\Delta_{R1}H_{0K}$ of (-108.9 ± 5.6) kJ mol⁻¹, which is in good agreement with recent *ab initio* calculations. In the ESI, parameterized forms for the output, $k_1(T,p)$, of the MESMER calculations are provided for a wide range of pressures and temperatures, for the bath gases helium, argon and nitrogen.

4 Acknowledgements

We are grateful to NERC for funding (NE/K005820/1) and the National Centre for Atmospheric Science. D. Medeiros acknowledges support from the Brazilian National Council for Scientific and Technological Development (CNPq, grant number 206527/2014-4).

5. Supporting Information Available

The supporting information contains Figure S1, parametrized forms for $k_1(T,p)$, for a range of buffer gases and the input file for the MESMER master equation analysis.

REFERENCES

1. D. Fowler, K. Pilegaard, M. A. Sutton, P. Ambus, M. Raivonen, J. Duyzer, D. Simpson, H. Fagerli, S. Fuzzi, J. K. Schjoerring and et al., *Atmospheric Environment*, 2009, **43**, 5193-5267.
2. M. L. Wesely, D. R. Cook, R. L. Hart and R. E. Speer, *J. Geophys. Res., D: Atmos.*, 1985, **90**, 2131-2143.
3. M. A. Blitz, R. J. Salter, D. E. Heard and P. W. Seakins, *J. Phys. Chem. A*, 2017, **121**, 3175-3183.
4. M. A. Blitz, R. J. Salter, D. E. Heard and P. W. Seakins, *J. Phys. Chem. A*, 2017, **121**, 3184-3191.
5. V. M. Miriyala, P. Bhasi, Z. P. Nhlabatsi and S. Sitha, *J. Theor. Comput. Chem.*, 2017, **16**, 15.
6. B. Long, J. L. Bao and D. G. Truhlar, *Phys. Chem. Chem. Phys.*, 2017, **19**, 8091-8100.
7. D. C. McCabe, S. S. Brown, M. K. Gilles, R. K. Talukdar, I. W. M. Smith and A. R. Ravishankara, *J. Phys. Chem. A*, 2003, **107**, 7762-7769.
8. D. C. McCabe, I. W. M. Smith, B. Rajakumar and A. R. Ravishankara, *Chem. Phys. Lett.*, 2006, **421**, 111-117.
9. D. R. Glowacki, C.-H. Liang, C. Morley, M. J. Pilling and S. H. Robertson, *J. Phys. Chem. A*, 2012, **116**, 9545-9560.
10. MESMER (Master Equation Solver for Multi-Energy Well Reactions); an Object Oriented C++ Program Implementing Master Equation Methods for Gas Phase Reactions with Arbitrary Multiple Wells., <https://www.chem.leeds.ac.uk/mesmer.html>, Accessed 2018.
11. D. R. Glowacki, C. H. Liang, C. Morley, M. J. Pilling and S. H. Robertson, *J. Phys. Chem. A*, 2012, **116**, 9545-9560.
12. M. J. Pilling and S. H. Robertson, *Annual Review of Physical Chemistry*, 2003, **54**, 245-275.
13. Y. Zhao and D. G. Truhlar, *Theor. Chem. Acc.*, 2008, **120**, 215-241.
14. T. H. Dunning, *Journal of Chemical Physics*, 1989, **90**, 1007-1023.
15. R. A. Kendall, T. H. Dunning and R. J. Harrison, *Journal of Chemical Physics*, 1992, **96**, 6796-6806.
16. D. E. Woon and T. H. D. Jr., *The Journal of Chemical Physics*, 1993, **98**, 1358-1371.
17. K. A. Peterson, D. E. Woon and T. H. Dunning, *The Journal of Chemical Physics*, 1994, **100**, 7410-7415.
18. A. K. Wilson, T. van Mourik and T. H. Dunning, *Journal of Molecular Structure: THEOCHEM*, 1996, **388**, 339-349.
19. M. J. Frisch, G. W. Trucks, H. B. Schlegel, G. E. Scuseria, M. A. Robb, J. R. Cheeseman, G. Scalmani, V. Barone, B. Mennucci, G. A. Petersson, H. Nakatsuji, M. Caricato, X. Li, H. P. Hratchian, A. F. Izmaylov, J. Bloino, G. Zheng, J. L. Sonnenberg, M. Hada, M. Ehara, K. Toyota, R. Fukuda, J. Hasegawa, M. Ishida, T. Nakajima, Y. Honda, O. Kitao, H. Nakai, T. Vreven, J. A. Montgomery, J. E. Peralta, F. Ogliaro, M. Bearpark, J. J. Heyd, E. Brothers, K. N. Kudin, V. N. Staroverov, R. Kobayashi, J. Normand, K. Raghavachari, A. Rendell, J. C. Burant, S. S. Iyengar, J. Tomasi, M. Cossi, N. Rega, J. M. Millam, M. Klene, J. E. Knox, J. B. Cross, V. Bakken, C. Adamo, J. Jaramillo, R. Gomperts, R. E. Stratmann, O. Yazyev, A. J. Austin, R. Cammi, C. Pomelli, J. W. Ochterski, R. L. Martin, K. Morokuma, V. G. Zakrzewski, G. A. Voth, P. Salvador, J. J. Dannenberg, S. Dapprich, A. D. Daniels, Farkas, J. B. Foresman, J. V. Ortiz, J. Cioslowski and D. J. Fox, Wallingford CT2009.
20. X. S. Li and M. J. Frisch, *J. Chem. Theory Comput.*, 2006, **2**, 835-839.
21. K. Raghavachari, G. W. Trucks, J. A. Pople and M. Headgordon, *Chem. Phys. Lett.*, 1989, **157**, 479-483.
22. S. Sharma, S. Raman and W. H. Green, *J. Phys. Chem. A*, 2010, **114**, 5689-5701.
23. T. Baer and W. L. Hase, *Unimolecular Reaction Dynamics: Theory and Experiments*, Oxford University Press, New York, 1996.
24. J. W. Davies, N. J. B. Green and M. J. Pilling, *Chem. Phys. Lett.*, 1986, **126**, 373-379.
25. J. T. Bartis and B. Widom, *Journal of Chemical Physics*, 1974, **60**, 3474-3482.
26. W. H. Miller, *Journal of the American Chemical Society*, 1979, **101**, 6810-6814.

27. W. Klopper, D. P. Tew, N. Gonzalez-Garcia and M. Olzmann, *J. Chem. Phys.*, 2008, **129**, 114308/114301-114308/114307.
28. M. A. Blitz, K. J. Hughes and M. J. Pilling, *J. Phys. Chem. A*, 2003, **107**, 1971-1978.
29. D. R. Glowacki, S. K. Reed, M. J. Pilling, D. V. Shalashilin and E. Martinez-Nunez, *Phys. Chem. Chem. Phys.*, 2009, **11**, 963-974.
30. I. W. M. Smith, *Chem. Soc. Rev.*, 1985, **14**, 141-160.
31. D. Fulle, H. F. Hamann and H. Hippler, *Phys. Chem. Chem. Phys.*, 1999, **1**, 2695-2702.
32. M. A. Blitz, K. J. Hughes, M. J. Pilling and S. H. Robertson, *J. Phys. Chem. A*, 2006, **110**, 2996-3009.
33. R. J. Shannon, M. A. Blitz, A. Goddard and D. E. Heard, *Nature Chemistry*, 2013, **5**, 745-749.
34. M. A. Blitz, N. J. B. Green, R. J. Shannon, M. J. Pilling, P. W. Seakins, C. M. Western and S. H. Robertson, *J. Phys. Chem. A*, 2015, **119**, 7668-7682.
35. E. E. Greenwald, S. W. North, Y. Georgievskii and S. J. Klippenstein, *J. Phys. Chem. A*, 2005, **109**, 6031-6044.
36. H. Somnitz, *Phys. Chem. Chem. Phys.*, 2004, **6**, 3844-3851.

Table 1. Comparison of the theoretical calculations and experimental study on the reaction OH + SO₂, R1. See Figure 1 for details of the species. All calculated energies are quoted with zero point energy added and are relative to OH + SO₂.

	vdW / kJ mol ⁻¹	TS / kJ mol ⁻¹	$\Delta_R H_{0K}(\text{HOSO}_2)$ / kJ mol ⁻¹	$\Delta_R H_{298K}(\text{HOSO}_2)$ / kJ mol ⁻¹
Miriyala <i>et al.</i> 2017 ⁵	-17.6	22.2	-109.2	
This study 2017	-7.2	1.2	-110.9	
Klopper <i>et al.</i> 2008 ²⁷			-109.4	-114.7 ± 3
Long <i>et al.</i> 2017 ⁶		1.1	-111.5	
Somnitz (2004) ³⁶			-103.6	
Blitz(2003) ²⁸				-113 ± 6

Table 2. MESMER fits to the experimental data on R1, where $\langle \Delta E_{\text{down}} \rangle = \Delta E_{\text{d}} \times (T/298)^m$.

	$\Delta_{\text{R1H0K}} / \text{kJ mol}^{-1}$	$\Delta E_{\text{d,He}} \times (T/298)^m / \text{cm}^{-1}$		$\Delta E_{\text{d,Ar}} \times (T/298)^m / \text{cm}^{-1}$		$\text{ILT}^{(a)} = A \times (T/298)^n$	TS/ kJ mol^{-1}	$\chi^2 / \text{pts}^{(b)}$
Vibration Model A	-112.2 ± 0.8	148 ± 15	1.0 fixed	319 ± 30	0.5 fixed	$1.6 \pm 1.9 \times 10^{-10}$	-0.38 ± 0.16	1.33
						0.56 ± 0.68		
Vibration Model B	-112.3 ± 0.8	152 ± 16	1.0 fixed	331 ± 33	0.5 fixed	1.6×10^{-10} fixed	-0.31 ± 0.13	1.31
						0.56 fixed		
Hindered Model C	-109.1 ± 0.8	122 ± 12	1.0 fixed	231 ± 20	0.5 fixed	$1.3 \pm 5.9 \times 10^{-10}$	-0.24 ± 0.10	1.33
						-0.80 ± 4.2		
Hindered Model D	-108.9 ± 0.7	120 ± 6	1.0 fixed	235 ± 11	0.5 fixed	1.3×10^{-10} fixed	-0.25 ± 0.08	1.31
						-0.80 fixed		
Hindered Model E	-108.9 ± 5.6	120 ± 24	0.99 +/- 1.52	233 ± 61	0.5 fixed	1.3×10^{-10} fixed	$-0.24 +/- 0.10$	1.32
						-0.80 fixed		
Model F	-112.6 ± 1.0	209 ± 17	1.0 fixed	350 ± 24	0.5 fixed	1.3×10^{-10} fixed	1.1 fixed	3.15
						-0.80		
Model G	-111.5 fixed	207 ± 16	1.0 fixed	350 ± 16	0.5 fixed	1.3×10^{-10} Fixed	1.1 fixed	3.27
						-0.80 fixed		
ILT(TS) Model H	-108.5 ± 0.9	114 ± 11	1.0 fixed	238 ± 20	0.5 fixed	$5.95 \pm 0.83 \times 10^{-13}$		1.30
						-0.11 ± 0.27		

^(a)Units are $\text{cm}^3 \text{ molecule}^{-1} \text{ s}^{-1}$, see main text for more information on ILT. ^(b)Number of points equals 36.

